JACS
JOURNAL OF THE AMERICAN CHEMICAL SOCIETY
Article
pubs.acs.org/JACS

Theoretical Investigation into the Mechanism of Au(I)-Catalyzed Reaction of Alcohols with 1,5 Enynes

Alireza Ariafard,*[,†] Esmat Asadollah,[†] Maryam Ostadebrahim,[†,§] Nasir Ahmad Rajabi,[†,∥] and Brian F. Yates*[,‡]

[†]Department of Chemistry, Faculty of Science, Central Tehran Branch, Islamic Azad University, Shahrak Gharb, Tehran, Iran
[§]Department of Chemistry, Shahre-Rey Branch, Islamic Azad University, Tehran, Iran
[∥]Department of Chemistry, Imam Khomeini International University, Qazvin, Iran
[‡]School of Chemistry, University of Tasmania, Private Bag 75, Hobart TAS 7001, Australia

Supporting Information

ABSTRACT: Density functional theory has been used to investigate the reactions of 1,5 enynes with alcohols in the presence of a gold catalyst. We have compared the mechanism of the alcohol addition reaction for the enyne with that of the enyne where the carbon at position 3 is replaced with silicon. We find that different intermediates are present in both cases, and in the case of the silicon analogue, the intermediate that we find from the calculations is different from any that have previously been proposed in the literature. For the silicon analogue we have been able to rationalize the observed effects of alcohol concentration and nucleophilicity on the product distribution. For the carbon-based enyne we have shown why different products are observed depending on the substitution at position 3 of the enyne. Overall, we have provided for the first time a consistent explanation and rationalization of several different experiments that have been previously published in the literature. Our mechanism will assist in predicting the outcome of experimental reactions involving different alcohols, reagent concentrations, and substitution patterns of the 1,5 enynes.

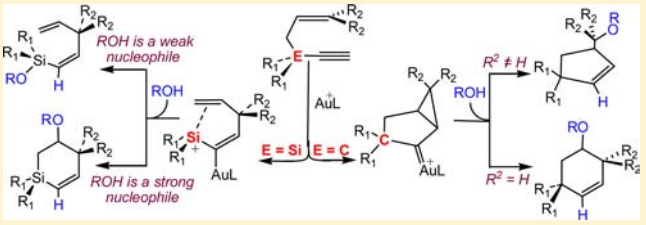

1. INTRODUCTION

It is well established that Au(I) catalysts are capable of activating enynes[1] toward reaction with alcohols.[2,3] For example, Toste et al. showed that 1,5 enyne **I** reacts with MeOH in the presence of Au(I) to give methoxycyclization product **II**.[4] Kozmin et al. subsequently reported that the intramolecular hydroxycyclization of 1,5 enynes with tethered nucleophiles by Au(I) (or Au(III)) takes place in a similar manner.[5] Another interesting type of methoxycyclization product (**IV**) was found by Gagosz et al. via the Au(I)-catalyzed reaction of MeOH with the 1,5 enynes **III** having substituent(s) at C6.[6] The intermediate **V** was proposed to be responsible for the formation of both the products **II** and **IV**; the attack of methanol at C^e gives **II**, while that at C^f gives **IV** (see Scheme 1).[4]

In contrast, replacing the carbon tether at the 3 position with a silicon atom[7] results in a change in the reaction mechanism. Park and Lee observed that Au(I)-catalyzed reaction of 1,5 enyne **VI** with ^{i}PrOH (1 equiv) affords alkenylsilane **VII**.[8] At the same time, Toste et al. investigated a similar reaction in the presence of a higher concentration of alcohols (3 equiv) and found that, depending on the nature of heteronucleophiles, different products are formed; when the heteronucleophile is PhOH, product **IX** is formed, and when the heteronucleophile is MeOH, product **X** is formed.[9] Several reaction mechanisms and intermediates (**XI**,**XII**) have been proposed to account for the formation of products **IX** (or **VII**) and **X**. Echavarren suggested that the formation of products may occur through the nucleophilic attack of ROH to either Si or C^e of bicyclic intermediate **XII**. Alternatively, either the ring expansion of **XII** or the 6-endo mode attack of the pendant alkene of substrate–gold complex[8] could generate intermediate **XII**. This intermediate (**XII**) can then be trapped by a ROH in either Si or C^e to give the corresponding products.[2,8,9] Another likely possibility for the formation of **IX** (or **VII**) is rearrangement of **XII** to the silyl cation **XIII** and then trapping of ROH by the Si cation (Scheme 2).[9] These observations prompted us to theoretically explore the reaction mechanism of gold-catalyzed alcohol addition to 1,5 enynes. Ongoing research is principally aimed at understanding how replacing the carbon tether at the 3-position with a silicon atom affects the mechanism of alcohol addition to 1,5 enynes. Accordingly, we need to find which intermediate(s) is formed during the course of the alcohol addition reactions in the presence of a Au(I) catalyst. The dependency of the regioselectivity of the nucleophilic attack on the nature of ROH and substrate will be evaluated in this study.

Received: August 13, 2012
Published: September 19, 2012

dx.doi.org/10.1021/ja308038z | J. Am. Chem. Soc. 2012, 134, 16882–16890

Scheme 1

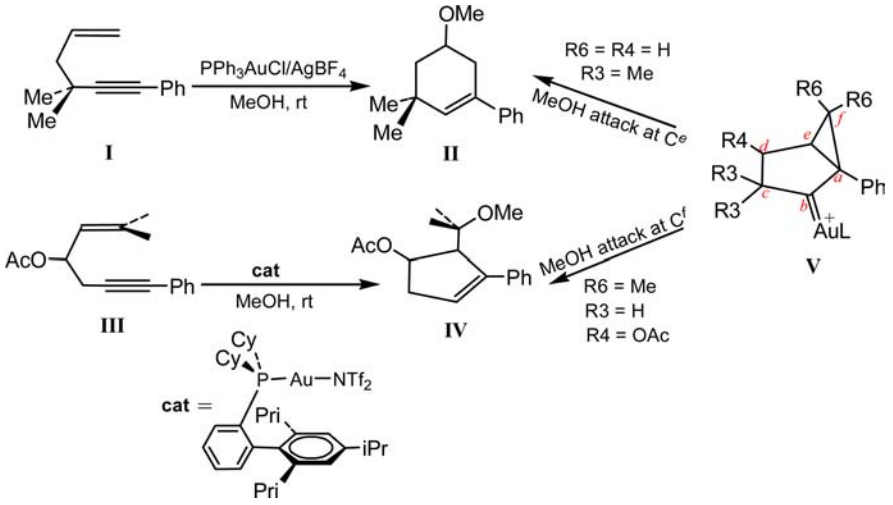

Scheme 2

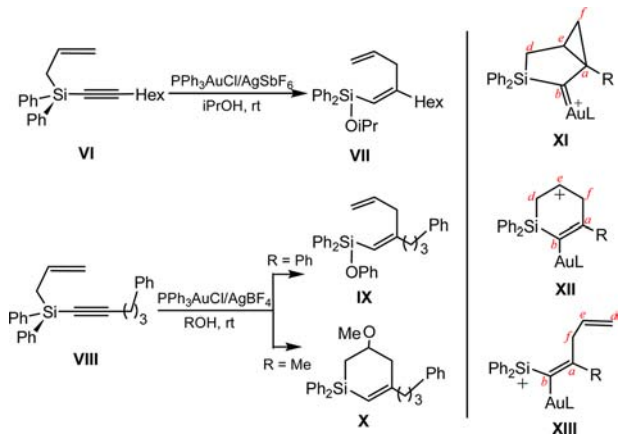

2. COMPUTATIONAL DETAIL

Gaussian 09[10] was used to fully optimize all the structures reported in this paper at the B3LYP level of density functional theory (DFT).[11] The effective core potential of Hay and Wadt with a double-ξ valence basis set (LANL2DZ)[12] was chosen to describe Au. The 6-31G(d) basis set was used for other atoms.[13] A polarization function of ξ_f = 1.050 was also added to Au.[14] This basis set combination will be referred to as BS1. Frequency calculations were carried out at the same level of theory as for structural optimization (see Supporting Information). IRC[15] calculations were used to confirm the connectivity between transition structures and minima. Because recent studies have established that M06[16] predicts the activation energies more accurately than B3LYP,[17] we carried out single-point energy calculations for all the structures with a larger basis set (BS2) at the M06 level. BS2 utilizes the quadruple-ζ valence def2-QZVP[18] basis set on Au and the 6-311+G(2d,p) basis set on other atoms. The solvation energies were calculated using BS2 on gas-phase optimized geometries with the CPCM solvation model[19] using dichloromethane as solvent. To estimate the corresponding Gibbs free energies, ΔG, the entropy corrections were calculated at the B3LYP/BS1 level, adjusted by the method proposed by Okuno[20] and finally added to the M06/BS2 total energies. We have used the potential and Gibbs free energies obtained from the M06/BS2//B3LYP/BS1 calculations in dichloromethane throughout the paper unless otherwise stated. The partial atomic charges were calculated on the basis of natural bond orbital (NBO) analyses.[21] In this study, PMe_3 was used as a model for phosphine ligands. We also used the substrates **1_C** and **1_Si** to study the alcohol addition to enynes in the presence of a Au(I) catalyst.

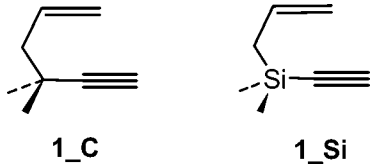

3. RESULTS AND DISCUSSION

The energy profiles for Au(I)-promoted intramolecular reaction between the alkene and alkyne groups of the 1,5 enynes **1_C** and **1_Si** are given in Figure 1. In the first step of these reactions, the substrates (**1_C** or **1_Si**) are assumed to be coordinated to the Au(I) catalyst, producing the adducts **2_C** or **2_Si.** In all the energy profiles the energy of the adduct is used as a reference point.

3.1. Nucleophilic Addition of the Pendant Olefin on the Alkyne Activated by Au(I) in 2_C. The nucleophilic attack of the pendant alkene onto the alkyne coordinated to $AuPMe_3^+$ in **2_C** through transition structure **1TS_C** ($\Delta G^{\ddagger}$ = 15.0 kcal mol^{-1}) leads to the formation of bicyclic intermediate **3_C** (Figure 1a). The reaction of **2_C** → **3_C** is calculated to be −3.1 kcal mol^{-1} exergonic. In supporting this result, other theoretical studies also showed the easy formation of bicyclic intermediates from 1,5 enynes.[22]

It is of interest to note that **3_C**, through the electron flow mechanism shown in Figure 1a, is capable of evolving to Au(I)-allene complex **4_C** with a reaction Gibbs energy of −1.8 kcal mol^{-1} by passing transition structure **2TS_C** ($\Delta G^{\ddagger}$ = 15.8 kcal mol^{-1}). This result is not surprising, considering that Horino and Toste proposed just one intermediate to account for cycloisomerization reactions of both 1,5-enyne and 1,4-enallene substrates.[23] The Gibbs activation barrier for the conversion of **4_C** to **3_C** is about 2.6 kcal/mol higher than that of **2_C** to **3_C**, explaining why the cycloisomerization of 1,4-enallenes requires slightly higher temperature than that of 1,5-enynes.[23]

3.2. Nucleophilic Addition of the Pendant Olefin on the Alkyne Activated by Au(I) in 2_Si. Our calculations show that the intramolecular reaction of the pendant alkene with the Au-bound alkyne in **2_Si** leads to formation of a different intermediate (Figure 1b). The IRC calculations confirm that transition structure **1TS_Si** with a Gibbs activation

dx.doi.org/10.1021/ja308038z | J. Am. Chem. Soc. 2012, 134, 16882−16890

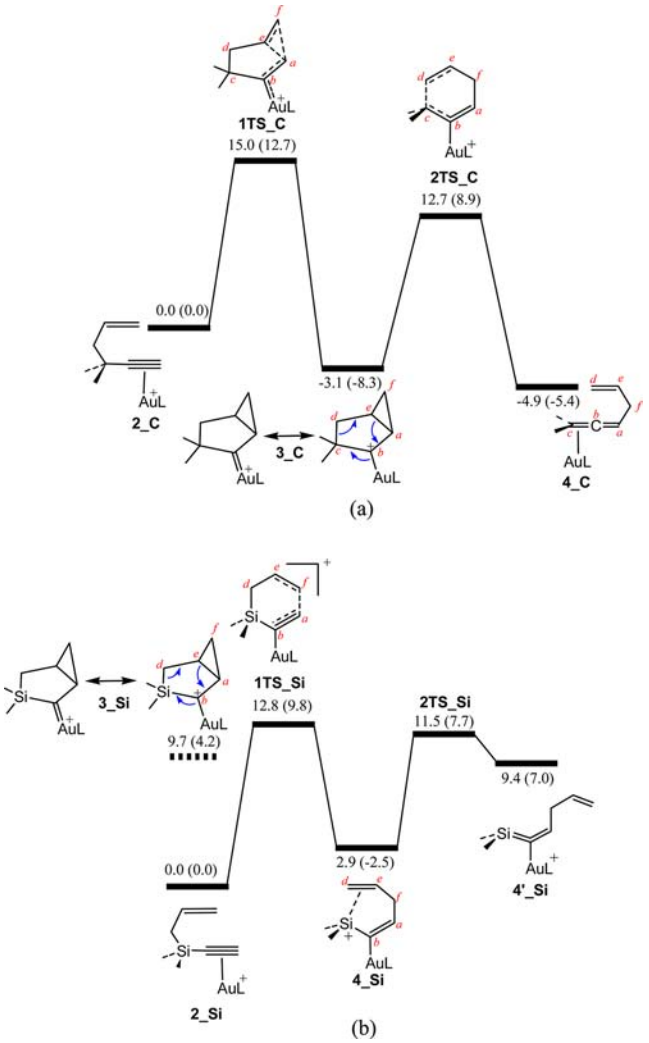

Figure 1. Energy profile calculated for nucleophilic addition of the pendant olefin on the alkyne activated by Au(I) in (a) **2_C** and (b) **2_Si**. The relative Gibbs and potential energies (in parentheses) obtained from the M06/BS2//B3LYP/BS1 calculations are given in kcal mol^{-1}.

barrier of 12.8 kcal mol^{-1} never leads to the bicyclic intermediate **3_Si** and instead is connected to intermediate **4_Si**. We noticed from computational searching that **3_Si** is not a local minimum. All attempts to locate this intermediate led to **4_Si**. In such a case, one can say that **2_Si** is only able to undergo a [3,3] isomerization and not a cycloisomerization reaction. This is opposite to what we obtained for **2_C**; in the case of **2_C**, the [3,3] isomerization reaction (formation of **4_C**) cannot occur directly and must certainly be preceded by a cycloisomerization reaction. This discrepancy could be due to the high polarity of Si−C^d bond in **3_Si**; we optimized **3_Si** by fixing the bond length of C^a−C^e at 1.590 Å and found that this fixed structure lies 9.7 kcal mol^{-1} above **2_Si**. The NBO calculations show that the Si−C^d bond in the partially optimized **3_Si** is strongly polarized toward the C^d atom (73.8% at C^d), while the C^c−C^d bond in **3_C** is predominantly covalent in character. The polarization of Si−C^d toward C^d causes the Si−C^d σ orbital to strongly interact with the C^a−C^e σ* orbital. This interaction pushes electron density away from C^e, promoting the electron flow mechanism shown in **3_Si** in Figure 1b and consequently does not allow the intermediate **3_Si** to be located as a local minimum.

We also found that **4_Si** gains a significant stability through the π-interaction between Si and the pendant alkene. The contribution of this π-interaction to the stability of the silyl cation **4_Si** is estimated to be nearly 6.6 kcal mol^{-1}. This estimation was obtained by optimization of a structure (**4′_Si**) in which the C^a−C^f bond of **4_Si** is rotated by 120°. The rotation results in lengthening of the Au−C^b bond by 0.082 Å

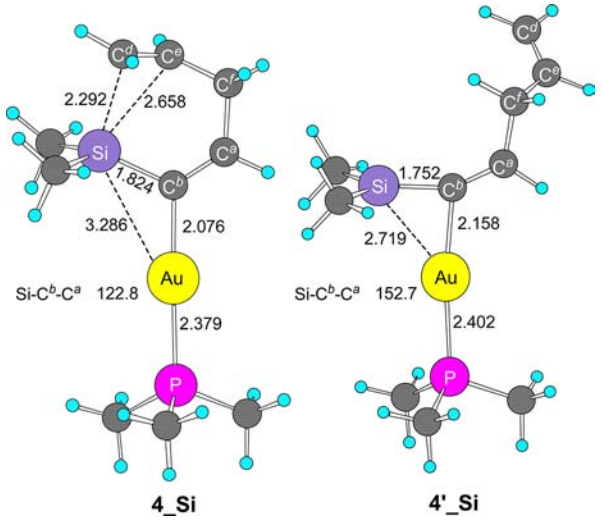

Figure 2. Optimized structures with selected structural parameters (bond lengths in Å) for **4_Si** and **4′_Si**.

as well as shortening of the Au−Si and Si−C^b bonds by 0.567 and 0.072 Å, respectively (Figure 2). This rotation is also accompanied by a widening of the Si−C^b−C^a bond angle by 29.9°. From these results one can propose two bonding

Scheme 3

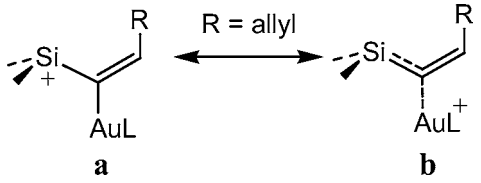

extremes for these two intermediates, silyl cation **a** and 1-silaallene **b** in Scheme 3. The bond length changes discussed above suggest that the participation of resonance form **b** in **4′_Si** is significant. In contrast, the interaction of the pendant alkene with Si in **4_Si** polarizes the weak Si−C^b π bond toward C^b, thus considerably increasing the contribution of the **a** resonance form to **4_Si.**

According to our calculations, the cyclic intermediate **XII**, as introduced in the Introduction section, is not located as a stationary point on the potential energy surface (PES). In such a case, only the silyl cation intermediate (**4_Si**) should be responsible for the formation of products **IX** and **X**. Below, we will show how this silyl cation intermediate interacts with ROH to generate corresponding products.

3.3. Regioselective Nucleophilic Attack of ROH into 4_Si. The reaction of ROH with **4_Si** may split into two different pathways: either through the nucleophilic attack of ROH at Si followed by proton transfer from the OH group to

dx.doi.org/10.1021/ja308038z | J. Am. Chem. Soc. 2012, 134, 16882−16890

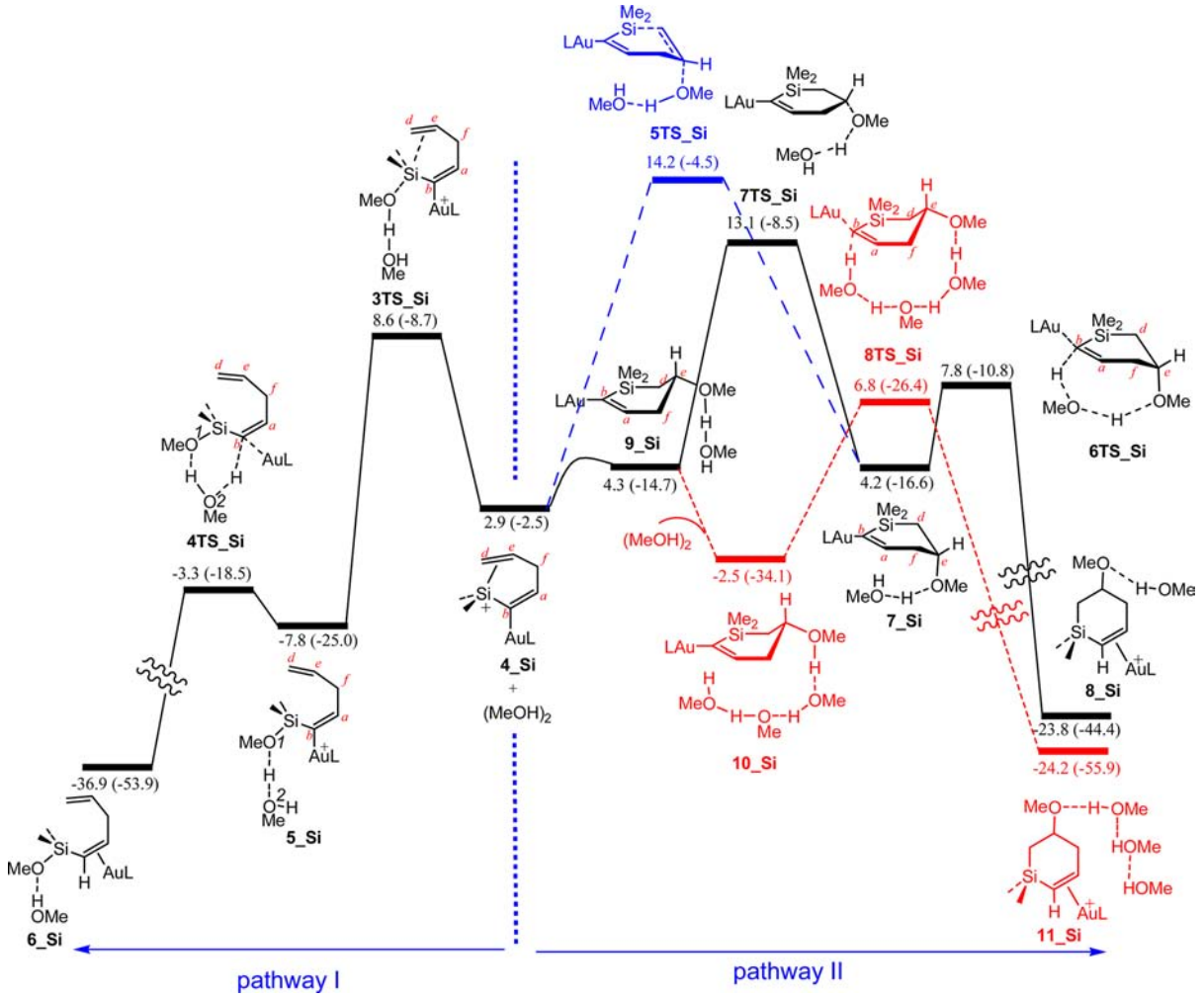

Figure 3. Energy profile calculated for regioselective nucleophilic addition of methanol to intermediate **4_Si**. The relative Gibbs and potential energies (in parentheses) obtained from the M06/BS2//B3LYP/BS1 calculations are given in kcal mol^{-1}.

C^b (pathway I) or through nucleophilic attack of ROH at C^e and subsequent proton transfer (pathway II) (Figure 3). Recent theoretical studies have demonstrated that Au(I)-catalyzed alcohol addition reactions at least require two ROH molecules.[24] One of them acts as a nucleophile and the other as a proton shuttle. To follow this strategy in this study, we consider the H-bonded adduct of two ROH molecules as a model nucleophile for trapping the intermediates.[25]

*3.3.1. Regioselective Nucleophilic attack of MeOH into **4_Si** (Pathways I and II).* As presented in Figure 3, methanol can attack onto Si through transition structure **3TS_Si** giving intermediate **5_Si** in an exergonic process (ΔG = −10.8 kcal mol^{-1}). The π-interaction between Si and the pendant alkene is disrupted during the nucleophilic attack step; the distances between Si and C═C midpoint are calculated to be 2.386, 2.526, and 4.216 Å in **4_Si**, **3TS_Si**, and **5_Si**, respectively. The proton transfer in **5_Si** occurs by hydrogen migration from O^1 to O^2 and then from O^2 to C^b (Figure 3). The Gibbs activation barrier and exergonicity for this step are computed to be 4.5 and 28.7 kcal mol^{-1}, respectively. Our calculations predict that the nucleophilic attack of MeOH into Si should be slower than the proton transfer.

There are two possible pathways (IIa and IIb) for the approach of MeOH toward C^e. In pathway IIa, MeOH attacks

Scheme 4

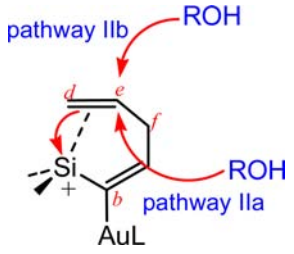

at C^e from the same side of the Au catalyst, whereas in pathway IIb it attacks from the opposite side of the catalyst (Scheme 4).

The attack via pathway IIa passes through transition structure **5TS_Si** with an overall activation barrier of 14.2 kcal mol^{-1} giving intermediate **7_Si** (Figure 3). In comparison, the attack via pathway IIb occurs in a barrierless fashion and leads to the formation of **9_Si**. This suggests that the nucleophilic attack via pathway IIa is much more energy consuming than that via pathway IIb. This is because a smaller orbital overlap is predicted to exist between C^d and Si in **5TS_Si**; C^d asymmetrically approaches Si in **5TS_Si** as evidenced by a much larger angle for H^2−C^d−Si than for H^1−C^d−Si (Scheme 5). In contrast, during the approach of methanol to C^e via pathway IIb, C^d starts interacting with Si in a symmetric

dx.doi.org/10.1021/ja308038z | J. Am. Chem. Soc. 2012, 134, 16882−16890

Scheme 5

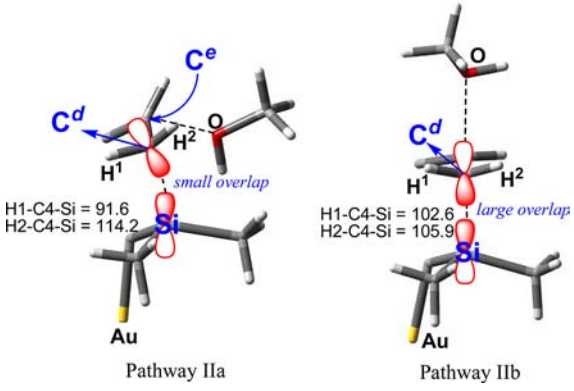

fashion, giving a maximum overlap between the C^e and Si p orbitals.

Both intermediates **7_Si** and **9_Si** are noticeably less stable than **5_Si** (Figure 3), indicating that the nucleophilic attack of MeOH to C^e is thermodynamically less favorable than that of Si. **7_Si** can directly undergo proton-transfer reaction via **6TS_Si** with a low activation barrier of 3.6 kcal mol^{-1}. This reaction which leads to the formation of the corresponding product is calculated to be exergonic by 28.0 kcal mol^{-1}. In contrast, our calculations show that it is impossible for **9_Si** to undergo the proton-transfer reaction due to a greater distance of the pendant methanol from C^b; the MeO^{2}H$\cdots C^b$ distances in **9_Si** and **7_Si** are 6.093 and 2.187 Å, respectively (Figure 4). In such a case, **9_Si** needs to isomerize to **7_Si** before the proton-transfer reaction. The isomerization of **9_Si** to **7_Si** occurs via transition structure **7TS_Si** with a global activation barrier of 13.1. This suggests that the isomerization is the rate-limiting step for pathway IIa. However, we found that the isomerization step can be omitted from the PES if at least two more methanol molecules are bonded to the pendant methanol of **9_Si**. The newly formed intermediate, **10_Si**, can now undergo the proton transfer via **8TS_Si** without isomerization with an overall activation barrier of 9.3 kcal mol^{-1} (Figure 3); the MeO^{4}H$\cdots C^b$ distance in **10_Si** is calculated to be 2.274 Å (Figure 4), a distance which is short enough in order for direct proton transfer to occur.

It appears from Figure 3 that the transition structure **3TS_Si** lies 1.8 kcal mol^{-1} higher than **8TS_Si** and 4.5 kcal/mol lower than **7TS_Si**. These results suggest that the nucleophilic attack of alcohols at C^e is energetically more favorable than that at Si if the necessary condition for the formation of a suitable intermediate such as **10_Si** is satisfied; otherwise the nucleophilic attack occurs at Si. We believe that the formation of such an intermediate, **10_Si**, is most likely if the concentration of alcohol is high enough. This claim could explain the experimental findings of Park and Lee[8] and Toste et al.[9] (Scheme 2). It can be inferred from these two works that the nucleophilic attack of alcohols in Park and Lee's experiment occurs at Si, while that for Toste's experiment occurs at C^e; Park and Lee used a 1:1 mixture of the alcohol and the enyne substrate, while Toste et al. used a 3:1 mixture.

*3.3.2. Regioselective Nucleophilic Attack of PhOH into **4_Si**.* We performed additional calculations using PhOH as a nucleophile to compare reactivity of PhOH with MeOH in trapping the silyl cation **4_Si**. A very similar reaction energy profile was obtained for the reaction of PhOH with **4_Si** (Figure 5). As mentioned above (Scheme 2), the reaction of 1,5 enyne **VI** with PhOH in the presence of Au(I) afforded alkenylsilane **IX** as the sole reaction product. Consistent with the experimental observations, we found that the nucleophilic attack of PhOH at Si (pathway I) is energetically more favorable than that of C^e (pathway II); **3TS_Si_Ph** lies below all the stationary points along pathway II (Figure 5). The reason for this can be explained in terms of the lower

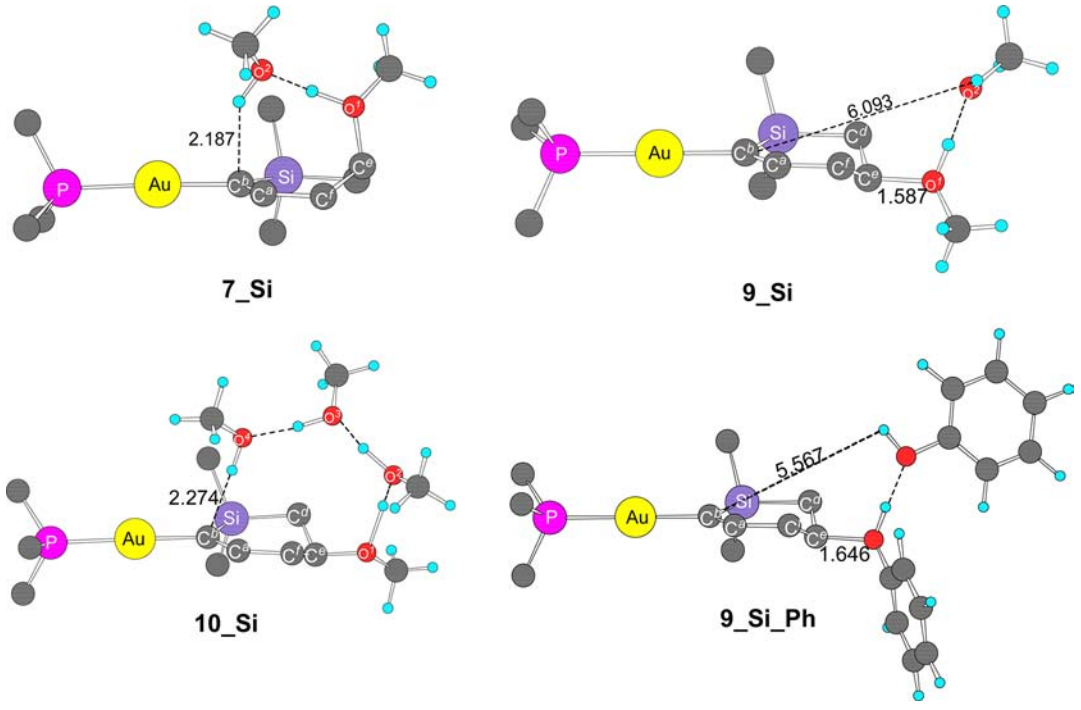

Figure 4. Optimized structures with selected structural parameters (bond lengths in Å) for **7_Si**, **9_Si**, **10_Si**, and **9_Si_Ph**. Hydrogen atoms (except for those on alcohols) have been omitted for clarity.

dx.doi.org/10.1021/ja308038z | J. Am. Chem. Soc. 2012, 134, 16882−16890

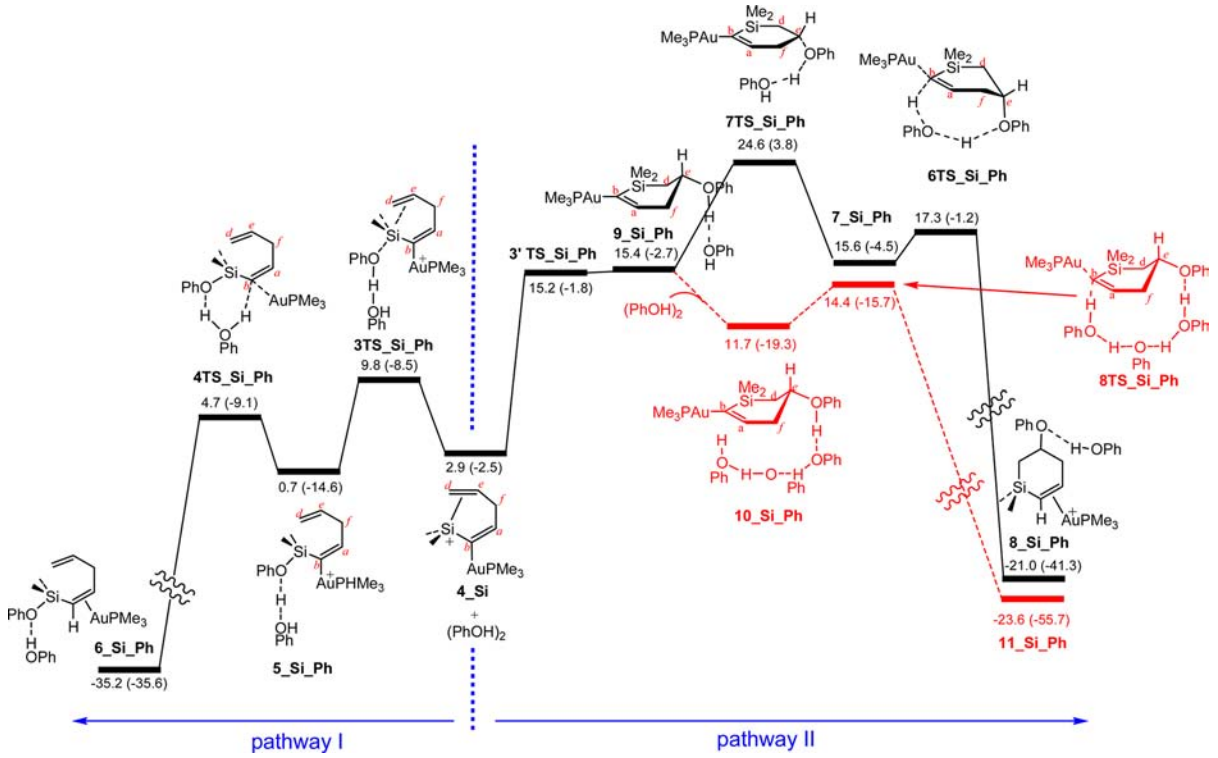

Figure 5. Energy profile calculated for regioselective nucleophilic addition of phenol to intermediate **4_Si**. The relative Gibbs and potential energies (in parentheses) obtained from the M06/BS2//B3LYP/BS1 calculations are given in kcal mol^{-1}.

nucleophilicity of PhOH as compared to MeOH. Indeed, the lower nucleophilicity of PhOH makes the conversion to **9_Si_Ph** much more endergonic than that to **9_Si**, causing the overall activation barrier for pathway II to increase. The lower nucleophilicity of PhOH is reflected in the longer C^e−O bond in **9_Si_Ph** than in **9_Si**; the C^e−O bond distance is calculated to be 1.646 and 1.588 Å in **9_Si_Ph** and **9_Si**, respectively (Figure 4).

3.4. Regioselective Nucleophilic Attack of MeOH into 3_C. As stated in the Introduction section, the attack of methanol on the bicyclic intermediate **3_C** can take place at either C^f (pathway III) or C^e (pathway IV). This step is calculated to be a rate-limiting step for both these pathways

Scheme 6

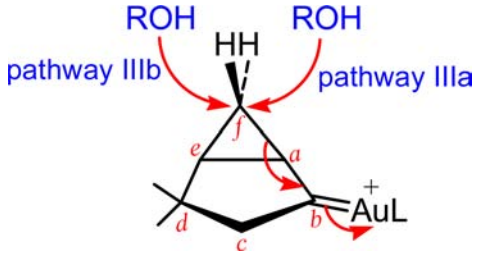

(Figure 6). Two alternative pathways are also possible for the attack of methanol at C^f (Scheme 6): the stereoselective nucleophilic attack from the same side of the Au catalyst (pathway IIIa) and from the opposite side of the Au catalyst (pathway IIIb). The stereoselective pathway IIIb is calculated to be energetically more favorable than pathway IIIa; transition structure **3TS_C** is lower in energy than **4TS_C** (Figure 6). The preference for pathway IIIb can be related to a greater

Scheme 7

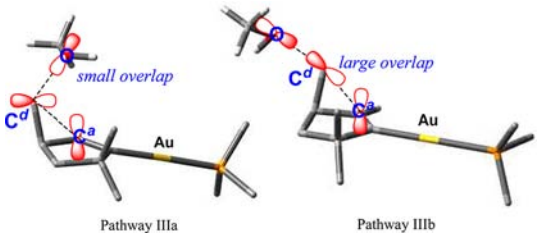

orbital overlap between C^f and O and between C^f and C^a in **3TS_C** (Scheme 7). The greater overlap is reflected in shorter C^f−O (2.134 Å) and C^f−C^a (1.980 Å) distances in **3TS_C**; the C^f−O and C^f−C^a distances in transition structure **4TS_C** are calculated to be 2.346 and 2.231 Å, respectively (Figure 7). Overcoming transition structure **3TS_C**, intermediate **4_C** is formed. This intermediate is not capable of undergoing the proton transfer and needs to isomerize to **5_C** in order for the pendant methanol to become closer to the C^b atom. **5_C** can now convert to the corresponding product in a very exergonic fashion via a transition structure in which the pendant methanol acts as a proton shuttle. This transition structure (**5TS_C**) lies 6.6 kcal mol^{-1} above **5_C**, suggesting that the proton transfer is an easy process.

In pathway IV, the activation barrier for methanol attack at C^e via transition structure **6TS_C** is found to be 15.6 kcal mol^{-1} (Figure 6). This attack results in intermediate **7_C**.[26] The isomerization of **7_C** to **8_C**, which brings the pendant methanol into the vicinity of C^b, takes place with an activation barrier of 5.2 kcal mol^{-1}. **8_C** can then undergo the proton transfer with an activation energy as low as 4.3 kcal mol^{-1} to produce the corresponding product.

dx.doi.org/10.1021/ja308038z | J. Am. Chem. Soc. 2012, 134, 16882−16890

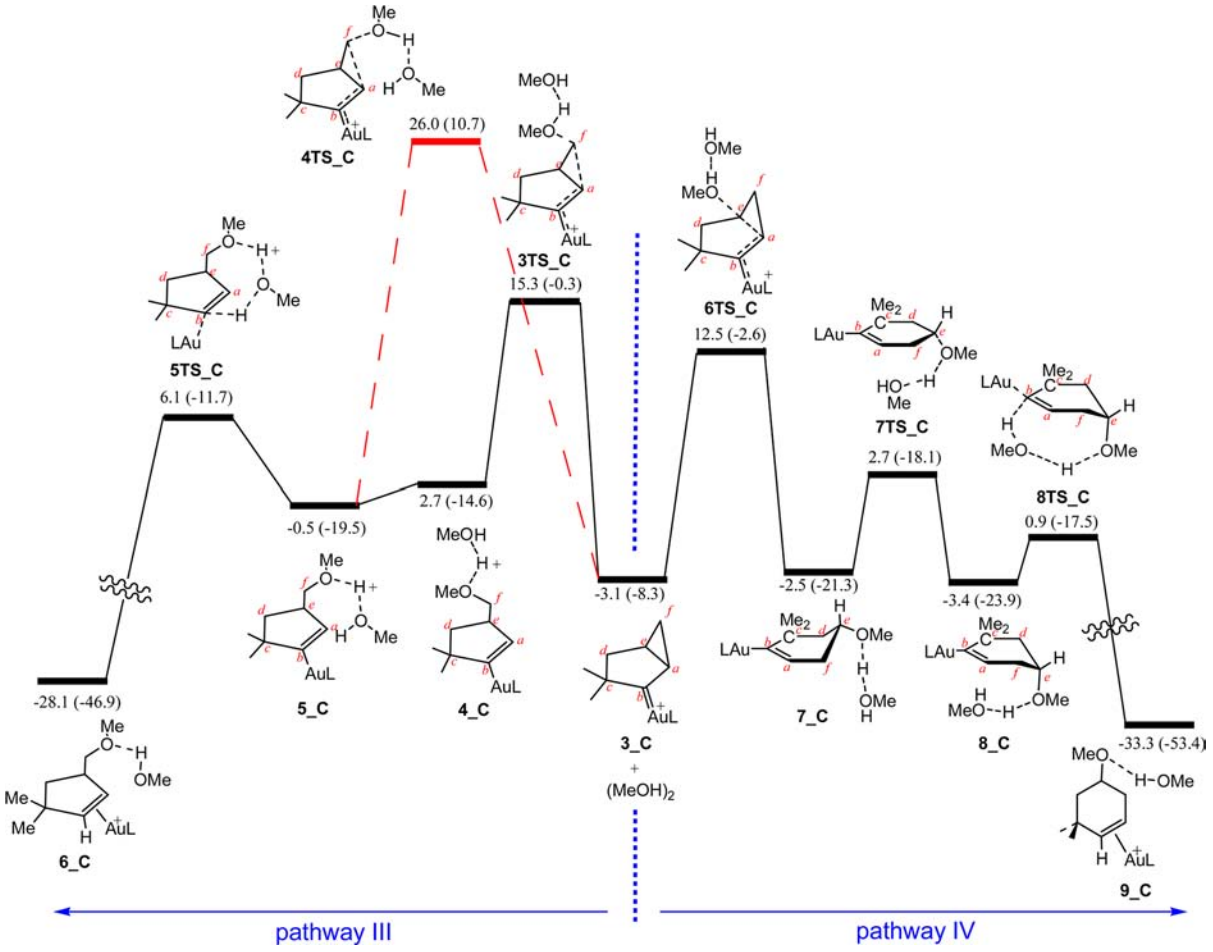

Figure 6. Energy profile calculated for regioselective nucleophilic addition of methanol to intermediate **3_C**. The relative Gibbs and potential energies (in parentheses) obtained from the M06/BS2//B3LYP/BS1 calculations are given in kcal mol^{-1}.

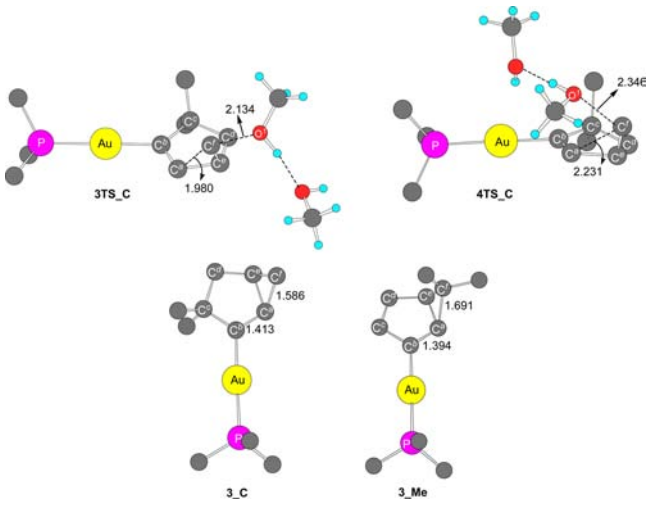

Figure 7. Optimized structures with selected structural parameters (bond lengths in Å) for **3TS_C**, **4TS_C**, **3_C**, and **3_Me**. Hydrogen atoms (except for those on alcohols) have been omitted for clarity.

As mentioned above, the activation barrier height of the initial attack of methanol at C^f or C^e is determining which product is finally formed. Transition structure **6TS_C** lies 2.8 kcal mol^{-1} below **3TS_C** (Figure 6), implying that the pathway IV is energetically preferred over pathway III. This result is consistent with the experimental data that the reaction of 1,5 enyne **I** with methanol leads to the formation of methoxycyclization product **II** (Scheme 1). However, as demonstrated by Gagosz et al. (Scheme 1), the substitution of the hydrogen atoms at C^f with methyl groups results in a change in the regioselectivity reaction. In such a case, the methanol clearly prefers to attack at C^e and not C^f. In excellent agreement with the experiment, our calculations for the model substrate **1_Me** (Figure 8) show that the transition structure for the methanol attack at C^f (**3TS_Me**) lies 5.3 kcal/mol below the transition structure for the methanol attack at C^e (**6TS_Me**).

Although the activation barrier to the methanol attack at C^e of **3_Me** (14.9 kcal mol^{-1}) and **3_C** (15.6 kcal mol^{-1}) is almost

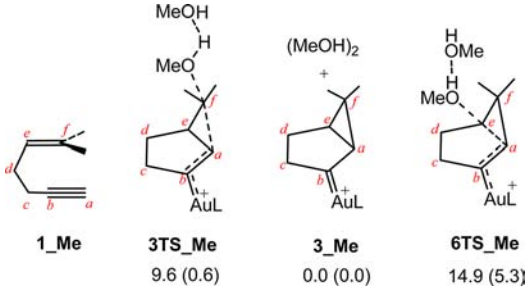

Figure 8. Relative Gibbs and potential energies (in parentheses) of **3TS_Me**, **3_Me**, and **6TS_Me**, in kcal mol^{-1}, obtained from the M06/BS2//B3LYP/BS1 calculations.

dx.doi.org/10.1021/ja308038z | J. Am. Chem. Soc. 2012, 134, 16882−16890

the same, that at C^f of **3_Me** is 8.8 kcal mol^{-1} lower in energy than that of **3_C**, indicating that the presence of two methyl substituents in **3_Me** renders the C^f atom more reactive toward the nucleophilic attack. Indeed, those two methyl substituents in **3_Me** increase the electrophilicity of C^f, as evidenced by a sufficient positive charge built-up at this atom; the partial NBO charge on C^f is calculated to be +0.084 and −0.351 in **3_Me** and **3_C**, respectively. Our calculations show that the C^f–C^a distance in **3_Me** is 0.105 Å longer than that in **3_C**, while the C^a–C^b distance in **3_Me** is 0.019 Å shorter than that in **3_C**. Based on these results, we believe that, in agreement with previous proposals,[22,27] the structures of **3_C** and **3_Me** can be described by a hybrid resonance between the two bonding extremes: carbenoid **c** and carbocation **d** (Scheme 8). Since the stability of the tertiary carbocations is much greater than the primary carbocations, the contribution of the carbocationic form **d** to the structure of **3_Me** is more significant. The increased participation of resonance form **d** in the bicyclic structure increases the electrophilic character of C^f, making it more susceptible to nucleophilic attack.

Scheme 8

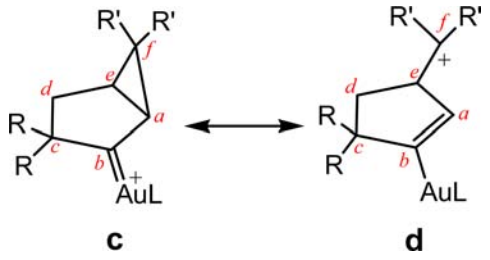

3.5. Summary of the Proposed Reaction Mechanisms. From the results of the calculations, we can summarize the mechanism for the Au(I)-catalyzed reaction of alcohols with enynes as follows (Scheme 9). For the enynes having a silicon atom at 3-position (Scheme 9a), the silyl cation **int_Si** is first formed in the presence of a Au(I) catalyst. This intermediate can then be trapped by the nucleophilic addition of an alcohol at either Si giving **P1_Si** or C^e giving **P2_Si**. Our calculations suggest that the nucleophilic addition at Si is favored if the concentration of alcohol is low enough or a ROH with a low nucleophilicity, such as PhOH, is used, otherwise the nucleophilic attack occurs at C^e. In contrast, for the enynes having a carbon atom at 3-position, the bicyclic intermediate **int_C** is definitely formed first (Scheme 9b). This intermediate is subsequently trapped by the nucleophilic attack of an alcohol at either C^e giving **P1_C** or C^f giving **P2_C**. The nucleophilic attack occurs at C^f if the substituents on C^f are not hydrogen, otherwise the attack takes place on C^e.

4. CONCLUSION

In this work, we have been able to rationalize, using DFT calculations, the different regioselectivities observed experimentally for the Au(I)-catalyzed addition of alcohols to 1,5-enynes. Specifically, our calculations support the notion that nucleophilic attack of the pendant alkene onto the alkyne, which is activated by coordination to Au(I), does not always lead to the formation of a bicyclic intermediate. In this regard, we find that the nature of the bond between atoms 3 and 4 plays a pivotal role in governing the structure of the ensuing intermediate. When the bond between atoms 3 and 4 is more ionic in character (i.e., with increasing negative charge on position 4), then the reactive intermediate is formed via a [3,3] isomerization process. In contrast, when the bond is more covalent in nature, a bicyclic intermediate is formed by way of a cycloisomerization reaction. In the context of this work, 1,5-enynes containing a silicon at position 3 undergo an initial [3,3] isomerization, affording a silyl cation and not a bicyclic species. The differing regioselectivity of the Au(I)-catalyzed addition of alcohols to 1,5-enynes is therefore attributed to the nature of the intermediates. Different reactive intermediates have different active sites toward the nucleophilic attack of ROH, thereby generating different products.

Scheme 9

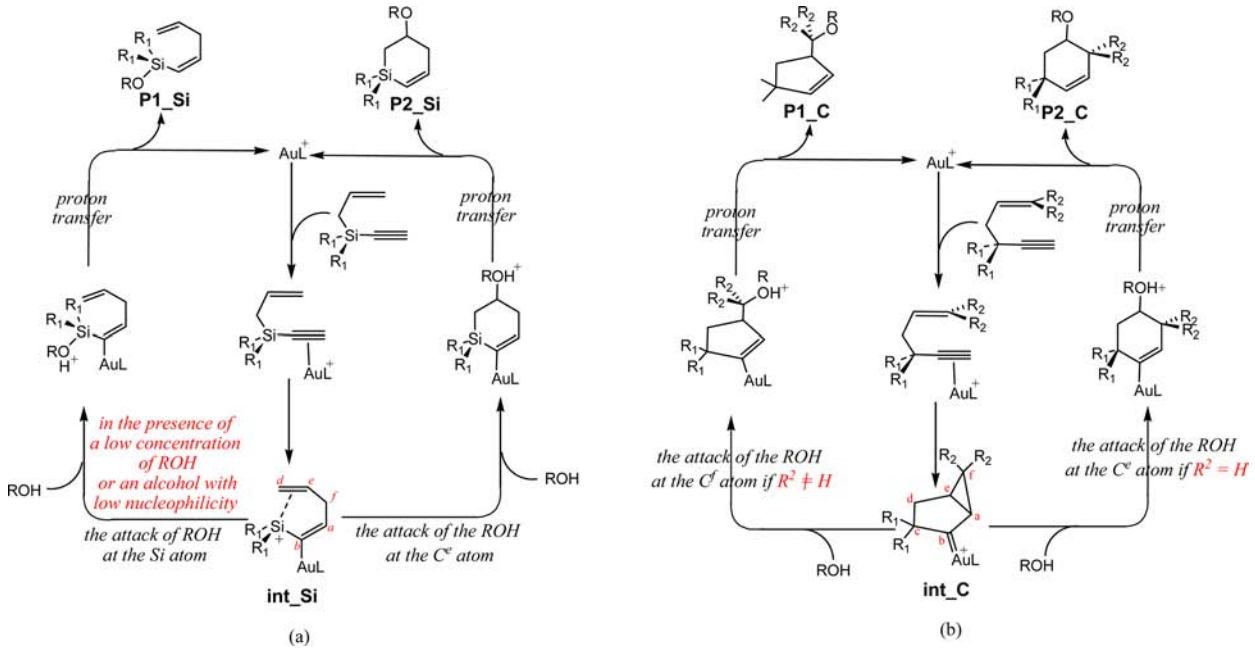

dx.doi.org/10.1021/ja308038z | J. Am. Chem. Soc. 2012, 134, 16882−16890

■ ASSOCIATED CONTENT

Supporting Information

Complete ref 10 and tables giving Cartesian coordinates of all optimized structures along with energies. This material is available free of charge via the Internet at http://pubs.acs.org.

■ AUTHOR INFORMATION

Corresponding Author

ariafard@yahoo.com; Brian.Yates@utas.edu.au

Notes

The authors declare no competing financial interest.

■ ACKNOWLEDGMENTS

We thank the Australian Research Council for financial support and the Australian National Computational Infrastructure and the University of Tasmania for computing resources. A.A., E.A., M.O., and N.A.R. are grateful to the financial supports of the Islamic Azad University, Central Tehran Branch. The authors also thank Prof. Agustí Lledós and Dr. Robert O'Reilly for their valuable advice during the completion of this study.

■ REFERENCES

(1) (a) Hashmi, A. S. K.; Frost, T. M.; Bats, J. W. *J. Am. Chem. Soc.* **2000**, *122*, 11553. (b) Luzung, M. R.; Markham, J. P.; Toste, F. D. *J. Am. Chem. Soc.* **2004**, *126*, 10858. (c) Nieto-Oberhuber, C.; López, S.; Muñoz, M. P.; Cárdenas, D. J.; Buñuel, E.; Nevado, C.; Echavarren, A. M. *Angew. Chem.* **2005**, *117*, 6302. (d) Nieto- Oberhuber, C.; López, S.; Jiménez-Núñez, E.; Echavarren, A. M. *Chem.—Eur. J.* **2006**, *12*, 5916. (e) Nieto-Oberhuber, C.; Pérez-Galán, P.; Herrero-Gómez, E.; Lauterbach, T.; Rodríguez, C.; López, S.; Bour, C.; Rosellón, A.; Cárdenas, D. J.; Echavarren, A. M. *J. Am. Chem. Soc.* **2008**, *130*, 269. (f) Soriano, E.; Marco-Contelles. *J. Acc. Chem. Res.* **2009**, *42*, 1026. (g) Hashmi, A. S. K.; Rudolph, M.; Huck, J.; Frey, W.; Bats, J. W.; Hamzic, M. *Angew. Chem., Int. Ed.* **2009**, *48*, 5848. (h) Shapiro, N. D.; Toste, F. D. *Synlett* **2010**, 675.

(2) (a) Jiménez-Núñez, E.; Echavarren, A. M. *Chem. Rev.* **2008**, *108*, 3326. (b) Muzart, J. *Tetrahedron* **2008**, *64*, 5815.

(3) (a) Nieto-Oberhuber, C.; Muñoz, M. P.; Buñuel, E.; Nevado, C.; Cárdenas, D. J.; Echavarren, A. M. *Angew. Chem., Int. Ed.* **2004**, *43*, 2402. (b) Nieto-Oberhuber, C.; Muñoz, M. P.; López, S.; Jiménez-Núñez, E.; Nevado, C.; Herrero-Gómez, E.; Raducan, M.; Echavarren, A. M. *Chem.—Eur. J.* **2006**, *12*, 1677.

(4) Gorin, D. J.; Sherry, B. D.; Toste, F. D. *Chem. Rev.* **2008**, *108*, 3351.

(5) Zhang, L.; Kozmin, S. A. *J. Am. Chem. Soc.* **2005**, *127*, 6962.

(6) Buzas, A. K.; Istrate, F. M.; Gagosz, F. *Angew. Chem., Int. Ed.* **2007**, *46*, 1141.

(7) For another example of a change in chemoselectivity by introducing a silyl group in the substrate see Hashmi, A. S. K.; Haufe, P.; Schmid, C.; Nass, A. R.; Frey, W. *Chem.—Eur. J.* **2006**, *12*, 5376.

(8) Park, S.; Lee, D. *J. Am. Chem. Soc.* **2006**, *128*, 10664.

(9) Horino, Y.; Luzung, M. R.; Toste, F. D. *J. Am. Chem. Soc.* **2006**, *128*, 11364.

(10) Frisch, M. J. et al. *Gaussian 09*, revision A.02; Gaussian, Inc.: Wallingford, CT, 2009.

(11) (a) Lee, C. T.; Yang, W. T.; Parr, R. G. *Phys. Rev. B* **1988**, *37*, 785. (b) Miehlich, B.; Savin, A.; Stoll, H.; Preuss, H. *Chem. Phys. Lett.* **1989**, *157*, 200. (c) Becke, A. D. *J. Chem. Phys.* **1993**, *98*, 5648.

(12) (a) Hay, P. J.; Wadt, W. R. *J. Chem. Phys.* **1985**, *82*, 270. (b) Wadt, W. R.; Hay, P. J. *J. Chem. Phys.* **1985**, *82*, 284.

(13) Hariharan, P. C.; Pople. *Theor. Chim. Acta J. A.* **1973**, *28*, 213.

(14) Ehlers, A. W.; Böhme, M.; Dapprich, S.; Gobbi, A.; Höllwarth, A.; Jonas, V.; Köhler, K. F.; Stegmann, R.; Veldkamp, A.; Frenking, G. *Chem. Phys. Lett.* **1993**, *208*, 111.

(15) (a) Fukui, K. *J. Phys. Chem.* **1970**, *74*, 4161. (b) Fukui, K. *Acc. Chem. Res.* **1981**, *14*, 363.

(16) (a) Zhao, Y.; Schultz, N. E.; Truhlar, D. G. *J. Chem. Theory Comput.* **2006**, *2*, 364. (b) Zhao, Y.; Truhlar, D. G. *J. Chem. Phys.* **2006**, *125*, 194101. (c) Zhao, Y.; Truhlar, D. G. *J. Phys. Chem. A* **2006**, *110*, 13126.

(17) Zhao, Y.; Truhlar, D. G. *Theor. Chem. Acc.* **2008**, *120*, 215.

(18) Weigend, F.; Furche, F.; Ahlrichs, R. *J. Chem. Phys.* **2003**, *119*, 12753.

(19) Barone, V.; Cossi, M. *J. Phys. Chem. A* **1998**, *102*, 1995.

(20) It is a method through which one can estimate the entropy difference between the gas and liquid phases. Okuno, Y. *Chem.—Eur. J.* **1997**, *3*, 212.

(21) Glendening, E. D.; Read, A. E.; Carpenter, J. E.; Weinhold, F. *NBO*, version 3.1; Gaussian, Inc.: Pittsburgh, PA, 2003.

(22) (a) Fan, T.; Chen, X.; Sun, J.; Lin, Z. *Organometallics* **2012**, *31*, 4221. (b) Soriano, E.; Marco-Contelles, J. *J. Org. Chem.* **2012**, *77*, 6231. (c) López-Carrillo, V.; Huguet, N.; Mosquera, Á; Echavarren, A. M. *Chem.—Eur. J.* **2011**, *17*, 10972. (d) Liu, Y.; Zhang, D.; Bi, S. *J. Phys. Chem. A* **2010**, *114*, 12893. (e) Liu, Y.; Zhang, D.; Zhou, J.; Liu, C. *J. Phys. Chem. A* **2010**, *114*, 6164.

(23) Horino, Y.; Yamamoto, T.; Ueda, K.; Kuroda, S.; Toste, F. D. *J. Am. Chem. Soc.* **2009**, *131*, 2809.

(24) (a) Paton, R. S.; Maseras, F. *Org. Lett.* **2009**, *11*, 2237. (b) Zhang, J.; Shen, W.; Li, L.; Li, M. *Organometallics* **2009**, *28*, 3129. (c) Kovács, G.; Lledós, A.; Ujaque, G. *Organometallics* **2010**, *29*, 3252. (d) Kovács, G.; Lledós, A.; Ujaque, G. *Organometallics* **2010**, *29*, 5919.

(25) A similar proton transfer via a water bridge network was explored by Hashmi and coworkers in a study on hydration of alkynes catalyzed by Au(I). See Krauter, C. M.; Hashmi, A. S. K.; Pernpointer, M. *ChemCatChem* **2010**, *2*, 1226.

(26) If we assume that the 1,4-enallene complex **4_C** is formed from **3_C** (Figure 1), then one can imagine that an alternative pathway for the formation of **7_C** can be the nucleophilic attack of methanol at C^e of this intermediate (Figure 1). All our attempts to locate a transition structure connecting **4_C** to **7_C** led to **6TS_C**. This implies that a direct methanolysis of the allene complex **4_C** is not operative, and in order for the reaction to occur, **4_C** should first convert to **3_C** and then methanol addition takes place at C^e of **3_C**.

(27) (a) Benítez, D.; Shapiro, N. D.; Tkachouk, E.; Wang, Y.; Goddard, W. A., III; Toste, F. D. *Nat. Chem* **2009**, *1*, 482. (b) Echavarren, A. M. *Nat. Chem.* **2009**, *1*, 431.